Geomechanics and Engineering, *Vol. 12, No. 1 (2017) 161-183*
DOI: https://doi.org/10.12989/gae.2017.12.1.161

Structural damage detection through longitudinal wave propagation using spectral finite element method

K. Varun Kumar [1a], T. Jothi Saravanan [2,3b], R. Sreekala [2c], N. Gopalakrishnan [*2,4] and K.M. Mini [1d]

[1] *Department of Civil Engineering, Amrita School of Engineering, Coimbatore, Amrita Vishwa Vidyapeetham, Amrita University, India*
[2] *Advanced Seismic Testing and Research Laboratory, CSIR-Structural Engineering Research Centre, Chennai-600113, India*
[3] *Department of Civil Engineering, The University of Tokyo, Tokyo- 1138654, Japan*
[4] *CSIR - Central Building Research Institute, Roorkee- 247667, India*

(*Received May 24, 2016, Revised September 20, 2016, Accepted September 30, 2016*)

Abstract. This paper investigates the damage identification of the concrete pile element through axial wave propagation technique using computational and experimental studies. Now-a-days, concrete pile foundations are often common in all engineering structures and their safety is significant for preventing the failure. Damage detection and estimation in a sub-structure is challenging as the visual picture of the sub-structure and its condition is not well known and the state of the structure or foundation can be inferred only through its static and dynamic response. The concept of wave propagation involves dynamic impedance and whenever a wave encounters a changing impedance (due to loss of stiffness), a reflecting wave is generated with the total strain energy forked as reflected as well as refracted portions. Among many frequency domain methods, the Spectral Finite Element method (SFEM) has been found suitable for analysis of wave propagation in real engineering structures as the formulation is based on dynamic equilibrium under harmonic steady state excitation. The feasibility of the axial wave propagation technique is studied through numerical simulations using Elementary rod theory and higher order Love rod theory under SFEM and ABAQUS dynamic explicit analysis with experimental validation exercise. Towards simulating the damage scenario in a pile element, dis-continuity (impedance mismatch) is induced by varying its cross-sectional area along its length. Both experimental and computational investigations are performed under pulse-echo and pitch-catch configuration methods. Analytical and experimental results are in good agreement.

Keywords: wave propagation; spectral finite element method; structural health monitoring; damage detection; ABAQUS

1. Introduction

The ability to monitor structures over their life time in order to ignore reliability and

∗Corresponding author, Director, E-mail: gnramana68@gmail.com
[a] Post Graduate Student, E-mail: kvkg124@gmail.com
[b] Doctoral Research Student, E-mail: tjs.saravanan@gmail.com
[c] Scientist, E-mail: kala@serc.res.in
[d] Professor, E-mail: k_mini@cb.amrita.edu

 ISSN: 2005-307X (Print), 2092-6219 (Online)

availability, and reduce life cycle costs is of vital importance in many engineering fields. The process of Structural Health Monitoring (SHM) includes monitoring the structure over time, obtaining the damage-sensitive features and analyzing the features to estimate the current state of system health (Farrar and Worden 2007). SHM has attracted significant worldwide research efforts because it provides engineers and infrastructure owners a more reliable way to monitor structural conditions for preventing catastrophic failure. SHM also provides quantitative data for designing reliable structures. Under extreme events like earthquakes or blast loadings, SHM provides real-time and reliable information about the performance of the structure. In general, the defect or damage can be defined as changes in the geometric or material properties of a structural system which adversely affects the performance of the system. Damage detection is carried out by monitoring the structure (Bently and Hatch 2003) through non-destructive testing (NDT) (Shull 2002) and damage prognosis methods (Farrar and Lieven 2007).

Among all NDT tools, wave propagation plays a vital role in identifying the damage. It is a transient dynamic phenomenon resulting from very short duration loadings like gust, birds hit, tool drops etc. which have very high-frequency content. The dynamic characteristics of the structures at high frequency are well understood with the help of wave propagation studies. Wave propagation based automatic SHM techniques are widely adopted in the nuclear and aerospace industry. But, these techniques are not in a well-matured state of development for civil engineering structures. Hence, enough importance is to be given in these areas of research so that an automatic alert and warning system can be designed for critical and important civil engineering structures. A coherent strategy for intelligent fault detection which includes precise definition, specification for operational evaluation, approach to sensor optimization and data processing methodology was described (Worden and Dulieu-Barton 2004).

Damage identification using the response of wave propagations are discussed in many kinds of literature (Gopalakrishnan and Doyle 1994, Palacz and Krawczuk 2002, Krawczuk *et al*. 2003, Palacz *et al*. 2005a, b, Krawczuk *et al*. 2006, Ostachowicz *et al*. 2006, Lee *et al*. 2007, Bityurin and Manzhosov 2009, Lakshmanan *et al*. 2010, Frikha *et al*. 2011, Guo and Yang 2012, Akbas 2014a, b, 2016, Gan *et al*. 2014, Bahrami and Teimourian 2015, Rao *et al*. 2015, Saravanan *et al*. 2015a, b, Gan *et al*. 2016). This is based on the assumption that the damages or discontinuities disturb the propagation of the waves in a structure. Wave propagation techniques are very effective because the waves travel for long range and depends on operating frequency, elastic properties of the material, material thickness, and density. The frequencies used in this method are usually higher than those used in the modal analysis. For assisting the damage detection, smart aggregate transducers like piezoelectric transducers and piezo ceramic wafer transducers are embedded in the concrete along with active sensing approach which generates and measures the stress wave propagation and thus damage is identified (Ai *et al*. 2016, and Feng *et al*. 2016). A review article of the buckling, bending, vibration and wave propagation of small-size beams is proposed and various research opportunities for future work are identified by Eltaher *et al*. 2016. Wavelet analysis of transient flexural wave is utilized to detect crack in beam by Tian *et al*. 2003. Kocatürk *et al*. (2011) demonstrated that the position and length of the part of dissimilar material can be attained by examining the supplementary secondary wave. For calculating axisymmetric wave propagation problems of anisotropic solids, a numerical algorithm on the method of characteristics is presented by Liu *et al*. (1997). Due to the presence of joints, non-uniformities, restrictions in boundary conditions and geometrics, the analysis of wave propagation in a framed structure is complicated and thus an effective modeling is required. Among all the methods, spectral finite element method is the best one for modeling (Gopalakrishnan and Doyle 1995). Numerical

investigations were carried out on an aluminum rod as well as the beam for illustrating the phenomena of axial wave propagation (Yang *et al*. 2016 and Ostachowicz 2008). Various analytical techniques are developed to handle wave propagation problems (Doyle 1997, Gopalakrishnan 2000, Krawczuk 2002, Mahapatra and Gopalakrishnan 2003, Kisa and Gurel 2007, Barbieri *et al*. 2009, Zak and Krawczuk 2011, Wu and Li 2014, He *et al*. 2014, He and Zhu 2015, Saravanan *et al*. 2016).

Pile foundation not only transfers load but also enables the construction activities in low bearing capacity soils and controls the level of soil settlement. The integrity of the pile is directly related to the safety of the super-structure. So, there is a need for monitoring the health and safety of pile from time to time. Early damage identification can provide a possibility of finding and repairing the defects. Many researchers used conventional finite element method for damage identification and needs to be explored. This paper deals with damage identification of a pile element (bar element) using axial wave propagation technique experimentally on four different concrete piles using Pulse echo configuration and Pitch catch configuration methods and this is also studied through numerical simulations using Spectral finite element method (SFEM), ABAQUS dynamic explicit analysis (Hibbitt *et al*. 2011) and the results are validated by experimental testing. In particular, detection of damage in form of discontinuity of cross-section is identified by analyzing wave speeds and reflections in the recorded velocity signals. The proposed damage models provided results compatible with experimentally measured signals.

2. Basics of wave propagation

When a structure is subjected to dynamic loads, it will experience the stresses of varying degrees of severity depending upon the magnitude of the load and its duration. If the variation of the load is of larger duration (order of seconds), the intensity of the load felt by the structure will be lower and such problems come under the category of structural dynamics. For those problems, two parameters namely natural frequency and normal mode shapes are significant. The main difference between wave propagation and classical structural dynamics arises due to higher frequency content in the primary case. Wave propagation is a transient phase of dynamic response before the on-going wave and the in-coming wave superimpose over each other to give a standing wave pattern. The ratio of reflected wave to the incident wave is controlled by the change in the impedance and hence the position of the damage and its magnitude could be quantified. Hence, wave propagation mechanics becomes handy for damage detection and diagnosis. Wave propagation through a prismatic bar element can be derived and the second order partial differential equation which governs the process can be written as

$$V_p{}^2 \frac{\partial^2 u}{\partial x^2} - \frac{\partial^2 u}{\partial t^2} = 0 \tag{1}$$

$$V_p = \sqrt{\frac{EA}{\rho A}} = \sqrt{\frac{E}{\rho}} \tag{2}$$

where u, x are displacement and co-ordinate in the longitudinal (axial) direction, V_p is phase velocity (also represented as 'c') in axial direction and E, ρ, A: Young's modulus, mass density and area of the rod (bar) element.

3. Experimental investigation

The experimental study for the phenomena of longitudinal wave propagation technique on axially loaded prismatic concrete pile element (considered as a free-free element) is described. The integrity of the pile for structural damage or discontinuities is judged by two methods namely pitch-catch configuration method and pulse-echo method. The structural damage is induced in the pile element by increasing and reducing the cross-sectional (c/s) area along the length and the location of the damage is varied. Four pile elements namely Pile1, Pile 2, Pile 3, and Pile 4 are casted using M30 grade concrete. The Pile 1 and Pile 3 are having symmetric damage (@ 2.5 m from head) and Pile 2 and Pile 4 are having un-symmetric damage (@ 4 m from head) as shown in Fig. 1. Consider, Wave speed, c = 3750 m/sec. All the concrete pile elements are of length 6 m and c/s of 0.2 m × 0.2 m is used for testing and are described as follows:

- Pile 1: The depth of the specimen-1 is 0.1 m for the center 1 m length (reduction in c/s area)
- Pile 2: The depth of the specimen-2 is 0.1 m for the center 1 m length from 1m from toe (reduction in c/s area)
- Pile3: The depth of the specimen-3 is 0.3 m for the center 1 m length (increase in c/s area)
- Pile 4: The depth of the specimen-4 is 0.3 m for the center 1 m length from 1m from toe (increase in c/s area)

When the pile head is struck by an impact load, the compression waves starts propagating with a wave speed (c) and reflects from pile tip and damages. When this initial wave encounters a change in the c/s (structural discontinuity) at a depth 'x', it reflects an upward traveling wave and it is observed at a time which is equal to twice the distance between the pile head and change in c/s divided by the velocity of the wave ($2x/c$). The stress wave inputs and wave reflections are measured as a function of time. For quick and reliable assessment of damage detection and identification, the velocity-time profiles are presented for the full time. From the time of reflection and phase velocity of the wave, the damage location can be obtained.

3.1 Pitch-catch configuration method

In this method, the accelerometer is attached to the pile top and bottom and the response of

Fig. 1 Four pile elements casted with different c/s

(a) Pitch-catch configuration set up

(b) Experimental set up

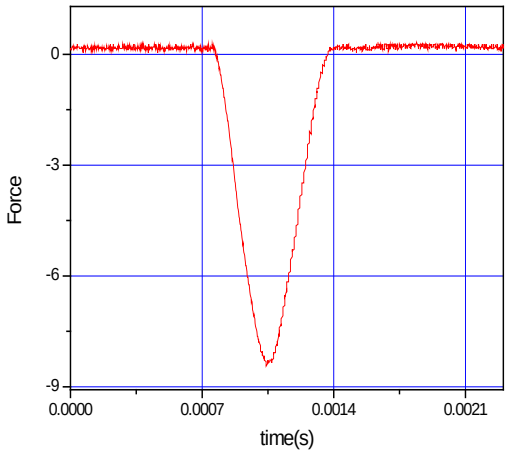

(c) Input excitation

Fig. 2 Experimental testing using pitch-catch configuration method

wave propagation is measured through the channels which are connected to cathode ray oscilloscope with special signal conditioning and A/D converter. An impulsive load is applied axially with the help of steel hammer tip as shown in Fig. 2. The acceleration response is obtained for each pile specimen and is shown in Fig. 3.

3.2 Pulse-echo method

In this method, the response of the pile elements under axial wave propagation technique is studied by using PIT (Pile integrity tester). A highly sensitive accelerometer is attached to the pile head with the help of viscous material and is connected to PIT analyzer. The experimental set up demonstrating the input excitation which was given at the head of the pile element is shown in Fig. 4. The velocity time profiles obtained from the PIT instrument are shown in Fig. 5. The Pile 1 and Pile 3 are considered to have symmetric damage (@ 2.5 m from head) and Pile 2 and Pile 4 are considered to have un-symmetric damage (@ 4 m from head) as shown in Fig. 1. The damage locations are calculated from the reflected times and are tabulated in Table 1. For the illustrated values, Pile 1, the location of damage is identified as 3.024 m instead of 2.5 m. Because, when the impact is given at head, the wave propagates such that it could not identify the damage which is

exactly at 2.5 m (the damage is very near to head). After few milliseconds, it identifies the reduced area at 3 m and same is the case for Pile 3. But, for Pile 2 and Pile 4 the damage locations are identified accurately as the damage location is at a far distance (4 m). From Fig. 5, it is clear that increased area shows negative velocity profile and reduced area shows positive velocity profile. The toe reflection is good for all the cases because it is approximately 6m (pile length).

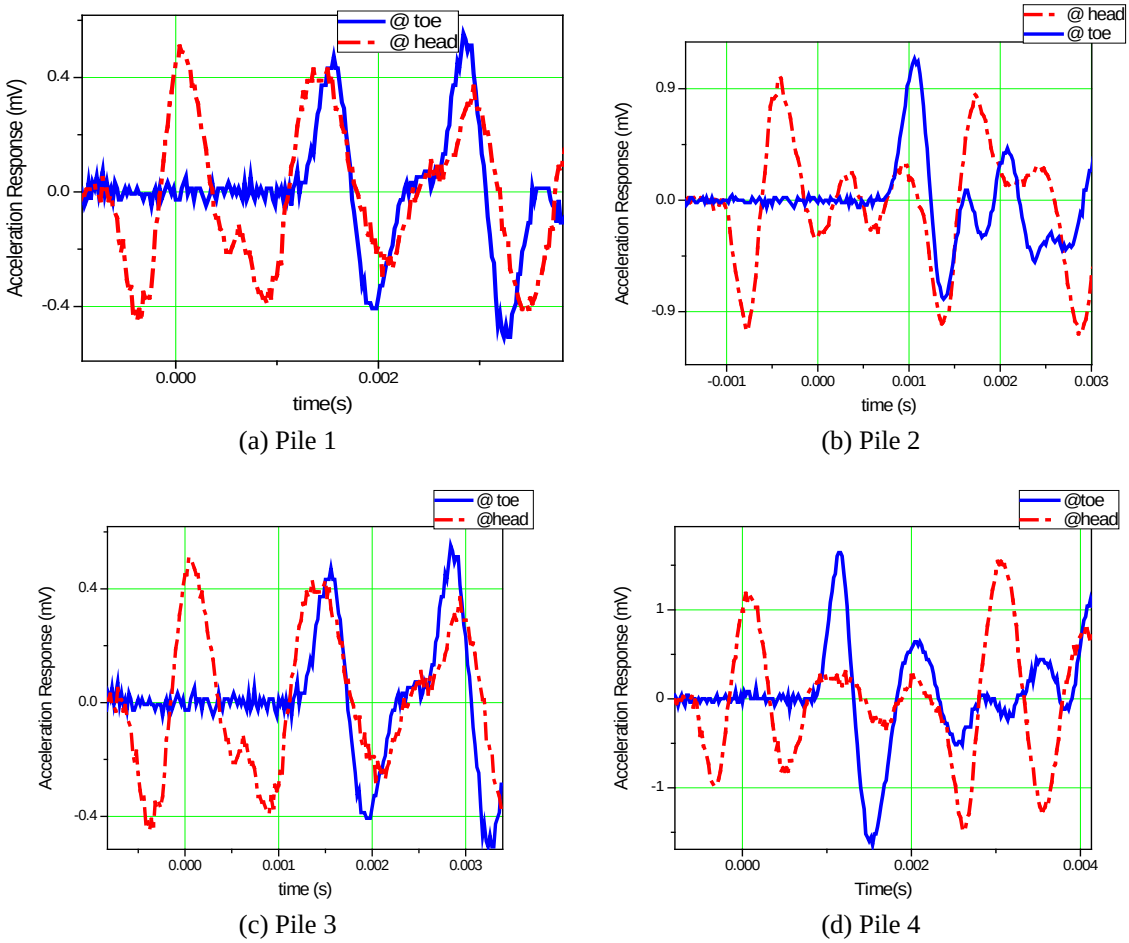

(a) Pile 1 (b) Pile 2

(c) Pile 3 (d) Pile 4

Fig. 3 Acceleration time response from pitch catch configuration method

Table 1 Damage locations identified by pulse-echo method

Specimen	Incident (ms)	Damage reflection (ms)	Location (m)	Toe reflection (ms)	Location (m)
Symmetry damage					
Pile 1	0.6	2.2133	3.024	3.6933	5.8
Pile 3	0.7	2.2133	2.837	3.7900	5.8
Un-Symmetry damage					
Pile 2	0.6	2.9800	4.087	3.7499	5.9
Pile 4	0.7	2.8376	4.008	3.8933	5.9

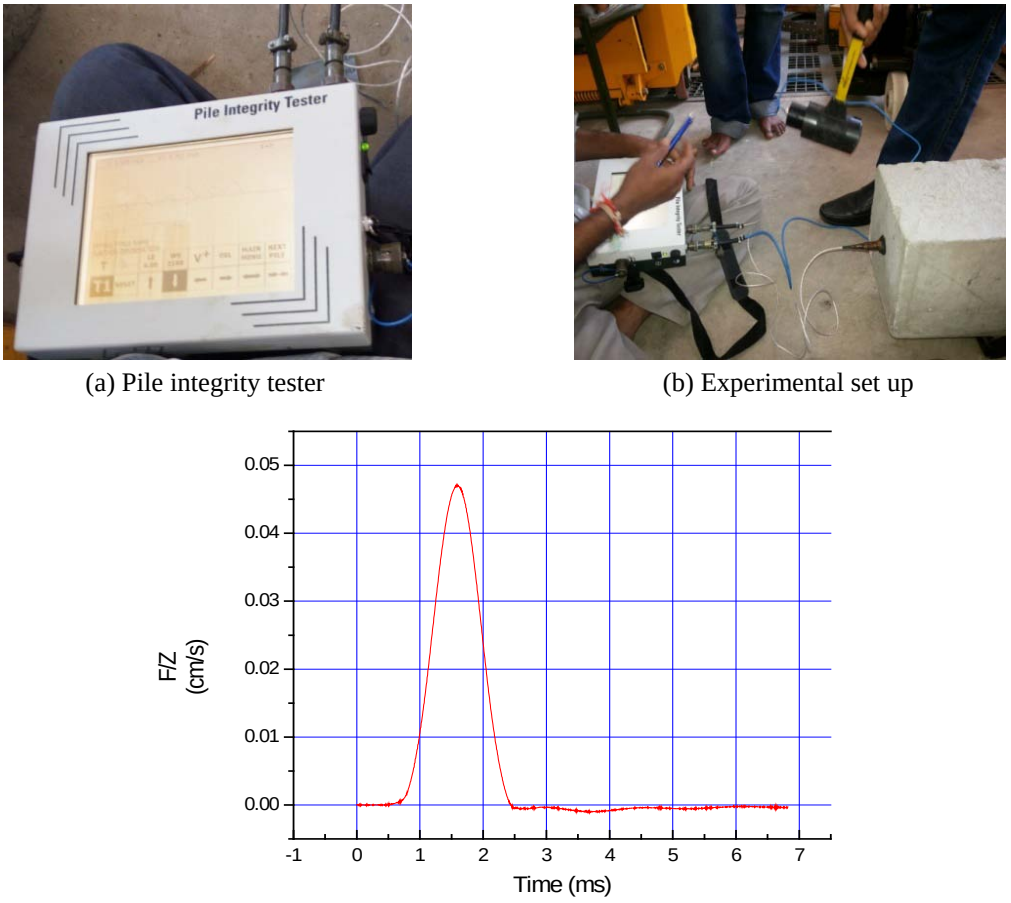

(a) Pile integrity tester (b) Experimental set up

(c) Input excitation

Fig. 4 Experimental Testing using PIT

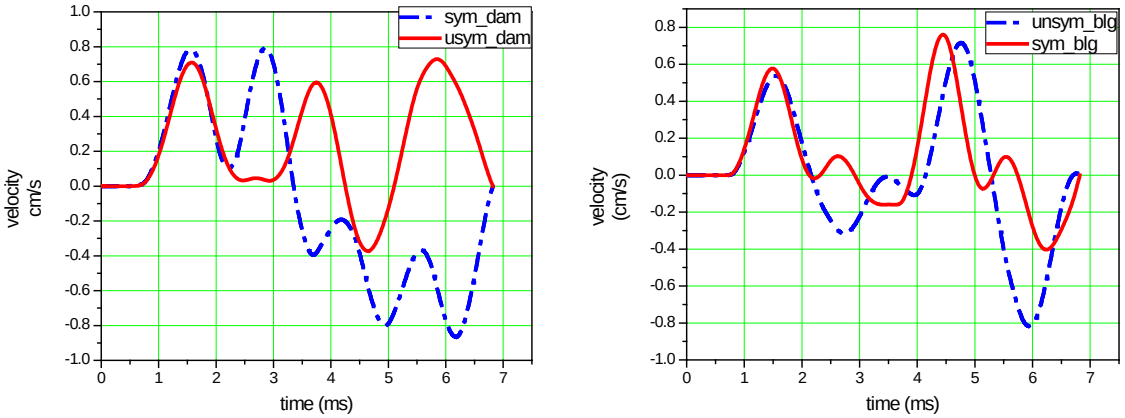

(a) (b)

Fig. 5 Velocity time responses obtained from pulse-echo method

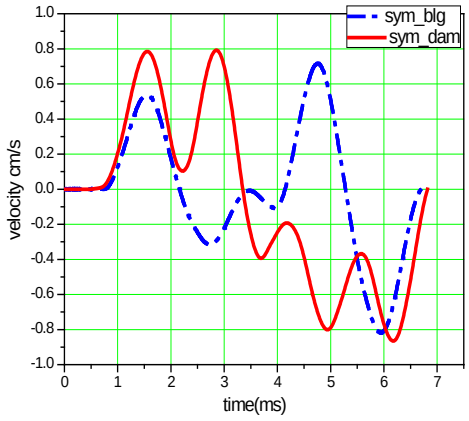

(c)

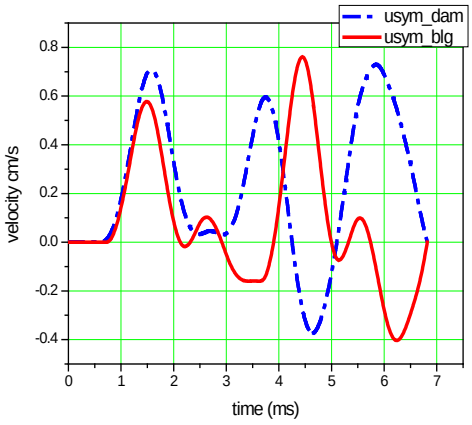

(d)

Fig. 5 Continued

4. Spectral Finite Element Method (SFEM)

For rods, beams, plates, and layered solids the spectral elements are readily available. Based on the elementary theory the spectral elements were readily developed for straight rod elements; however, modified axial deformation formulations based on Love theory are more appropriate for analyzing the wave propagation problems at higher frequencies. SFEM is a method in which the FFT algorithm is an essential part and gives problem sizes many orders smaller than conventional FEM.

4.1 Elementary theory

This theory assumes that at all the points of the c/s along the neutral axis, the axial deformations remains same and the transverse deformations are insignificant. The differential equation is given in Eq. (3) and with the boundary condition on u_o in Eq. (4)

$$EA\frac{\partial^2 u_o}{\partial x^2} - \rho A\frac{\partial^2 u_o}{\partial t^2} = 0 \tag{3}$$

$$F_u = EA\frac{\partial u_o}{\partial x} \tag{4}$$

where u_o – Displacement along the axial direction, E – Young's modulus, F_u – longitudinal force, A – area of the c/sand ρ – density of the material (rod). The dynamic stiffness matrices for a two node spectral element K_{df} and the throw-off element K_{dt} are shown in Eq. (5) (Doyle 1997)

$$K_{df} = \frac{ikEA}{(1-e^{-2ikL})}\begin{bmatrix} 1+e^{-2ikL} & -2e^{-ikL} \\ -2e^{-ikL} & 1+e^{-2ikL} \end{bmatrix}, \qquad K_{dt} = ikEA \tag{5}$$

Where, k is the wave number and is given as

$$k = \pm\sqrt{\frac{\rho\omega^2}{E}} \tag{6}$$

4.2 Love theory

Love theory is a one mode rod theory. When a rod is distorted longitudinally, due to Poisson's ratio effect it also contracts in transverse direction. So, for each particle of the rod there exists a transverse component of velocity. Nevertheless, the strain energy is the similar to the elementary rod theory and the kinetic energy is affected by supplementary terms (Doyle 1997).

The axial strain and transverse strain are connected to each other by $\epsilon_t = -v\epsilon$ consequently; the transverse velocity is specified by

$$\dot{u}_t = r\dot{\epsilon}_t = -vr\dot{\epsilon} = -vr\frac{\partial\dot{u}}{\partial x} \tag{7}$$

The transverse displacement is relative to the distance '*r*' from the centroid of the c/s. The total kinetic energy of the rod is given by

$$T = \int_{\forall}\frac{1}{2}\rho[\dot{u}(x,t)^2 + \dot{u}_t(x,t)^2]\,d\forall = \frac{1}{2}\int_0^L\int_A \rho\left[\dot{u}^2 + v^2r^2\left(\frac{\partial\dot{u}}{\partial x}\right)^2\right]dAdx \tag{8}$$

The total strain energy is given by

$$U = \frac{1}{2}\int_0^L EA\left(\frac{\partial u}{\partial x}\right)^2 dx \tag{9}$$

The potential of the applied forces is given by

$$V = -\int_0^L qdx - (-F_o u_o + F_L u_L) = -\int_0^L qdx - Fu\Big|_0^L \tag{10}$$

Substitute the above strain and potential energies into Hamilton's theorem, it gives the governing differential equation for $u(x,t)$ in Eq. (11) and with the boundary condition on u_o in Eq. (12)

$$EA\frac{\partial^2{}_{u_o}}{\partial x^2} + v^2\rho J\frac{\partial^2}{\partial x^2}\left(\frac{\partial^2 u_o}{\partial t^2}\right) - \rho A\frac{\partial^2 u_o}{\partial t^2} = 0 \tag{11}$$

$$F_u = EA\frac{\partial u_o}{\partial x} + v^2\rho J\frac{\partial}{\partial x}\left(\frac{\partial^2 u_o}{\partial t^2}\right) \tag{12}$$

The wave-number is given by the following relation

$$k = \pm\sqrt{\frac{\rho A\omega^2}{EA - v^2\rho J\omega^2}} \tag{13}$$

4.2.1 Rod spectral element for love theory

Using Love theory, the generation of dynamic stiffness matrix for a rod spectral element is focused in this section. Similar to elementary theory, the longitudinal displacement of a rod is given

$$\hat{u}(x) = Ae^{-ikx} + Be^{-ik(l-x)} \tag{14}$$

Applying boundary condition

$$\hat{u}_1(x=0) = A + Be^{-ikl}\,\hat{u}_2(x=L) = Ae^{-ikl} + B$$

Solving for constants A and B

$$A = \frac{\widehat{u_1} - \widehat{u_2}e^{-ikl}}{1-e^{-2ikl}} \qquad B = \frac{\widehat{u_2} - \widehat{u_1}e^{-ikl}}{1-e^{-2ikl}}$$

On substituting

$$\hat{u}(x) = \left[\frac{\widehat{u_1} - \widehat{u_2}e^{-ikl}}{1-e^{-2ikl}}\right]e^{-ikx} + \left[\frac{\widehat{u_2} - \widehat{u_1}e^{-ikl}}{1-e^{-2ikl}}\right]e^{-ik(l-x)} \tag{15}$$

$$\hat{u}(x) = \frac{\widehat{u_1}}{1-e^{-2ikl}}\left[e^{-ikx} - e^{-ik(2l-x)}\right] + \frac{\widehat{u_2}}{1-e^{-2ikl}}\left[-e^{-ik(x+l)} - e^{-ik(l-x)}\right] \tag{16}$$

The forces within the element in Eq. (12) can be expressed using formulas

$$\begin{aligned} F(x) &= EA\frac{\partial u}{\partial x} + v^2\rho J\frac{\partial \ddot{u}}{\partial x} \\ F(x) &= EA\left[A(-ik)e^{-ikx} + B(ik)e^{-ik(l-x)}\right] + v^2\rho J\,[[A(-ik)e^{-ikx} \\ &\quad + B(ik)e^{-ik(l-x)}]\,(-\omega^2)] \end{aligned} \tag{17}$$

On substituting for A and B

$$\begin{aligned} F(x) = \frac{ik}{1-e^{-2ikl}}\,[\,&EAu_1\left(-e^{-ikx} - e^{-ik(2l-x)}\right) + EAu_2\left(e^{-ik(x+l)} + e^{-ik(l-x)}\right) \\ &+v^2\rho J(-\omega^2)[u_1\left(-e^{-ikx} - e^{-ik(2l-x)}\right)] + v^2\rho J(-\omega^2)[u_2\left(e^{-ik(x+l)} + e^{-ik(l-x)}\right)] \end{aligned} \tag{18}$$

Put $x = 0$ in Eq. (18)

$$F(0) = \frac{ik}{1-e^{-2ikl}}\left[(-EA + v^2\rho J\omega^2)\left(1+e^{-2ikl}\right)u_1 + (-EA - v^2\rho J\omega^2)\left(2e^{-ikl}\right)u_2\right] \tag{19}$$

Put $x = l$ in Eq. (18)

$$F(l) = \frac{ik}{1-e^{-2ikl}}\left[(-EA + v^2\rho J\omega^2)\left(2e^{-ikl}\right)u_1 + (-EA - v^2\rho J\omega^2)\left(1+e^{-2ikl}\right)u_2\right] \tag{20}$$

The member loads at each end of the rod are connected to the displacements by

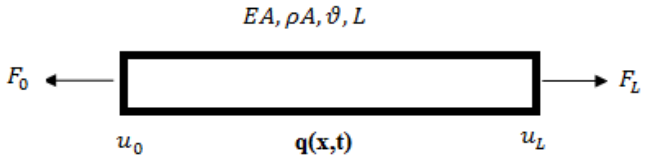

Fig. 6 Rod element with axial load

$$F_1 = -F(0), \qquad F_2 = +F(l)$$

This can be written in the form of $\{F\} = [k]\ \{u\}$ where $[k]$ is the frequency dependent dynamic element stiffness for the rod. It is symmetric as seen from the explicit matrix form

$$\begin{Bmatrix} F_1 \\ F_2 \end{Bmatrix} = \frac{ik}{1-e^{-2ikl}} \begin{bmatrix} (EA - v^2\rho J\omega^2)\left(1+e^{-2ikl}\right) & (EA + v^2\rho J\omega^2)\left(2e^{-ikl}\right) \\ (EA + v^2\rho J\omega^2)\left(2e^{-ikl}\right) & (EA - v^2\rho J\omega^2)\left(1+e^{-2ikl}\right) \end{bmatrix} \begin{Bmatrix} u_1 \\ u_2 \end{Bmatrix} \tag{21}$$

The square and symmetric matrix in this relation denotes the dynamic stiffness matrix K_{df} of the spectral element based on the Love theory.

$$K_{df} = \frac{ik}{(1-e^{-2ikL})} \begin{bmatrix} (EA - v^2\rho J\omega^2)\left(1+e^{-2ikL}\right) & -(EA - v^2\rho J\omega^2)2e^{-ikL} \\ -(EA - v^2\rho J\omega^2)2e^{-ikL} & (EA - v^2\rho J\omega^2)\left(1+e^{-2ikL}\right) \end{bmatrix} \tag{22}$$

4.3 SFEM for Pile (bar element) with discontinuities

Using SFEM, the axial wave propagation in rods is modeled for simulations. The amplitude of the external force is set as one of the responses obtained from the hammer hit. The specimen is discretized using SFEM and is shown in Fig. 7. For numerical analysis, the specimen is considered as bar element with free-free boundary conditions. The velocity of the wave (c) is 3750 m/s. The pitch-catch configuration is utilized for both the theories.

4.3.1 Results from Elementary theory

The response of velocity profiles obtained from the analytical study under elementary theory in SFEM is shown in Fig. 8 which shows the reflection of waves from the location of discontinuity and toe location and are in good agreement with the experimental results. Hence, SFEM identifies the location of structural discontinuities accurately.

4.3.2 Results from Love theory

The response of velocity profiles obtained from the analytical study under Love theory in SFEM is shown in Fig. 9 which clearly shows the reflection of waves from the location of discontinuity and toe location and gives better results when comparing to elementary theory. From numerical studies and Table 3, it is inferred that the time gap between the peaks of reflected pulse maintains a spatial difference of 1.5 m (4.0-2.5) and also maintains the damage length of 1m. The toe location and damage location are well identified (4 m and 2.5 m) with a slight variation. Thus the discontinuity location is identified numerically using SFEM.

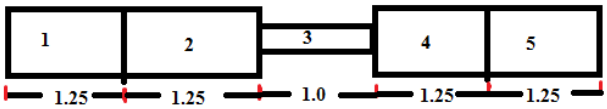

(a) Pile 1

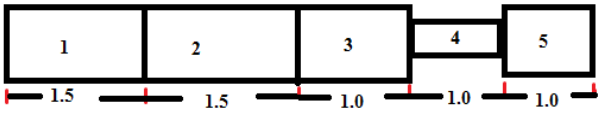

(b) Pile 2

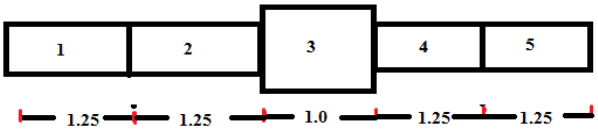

(c) Pile 3

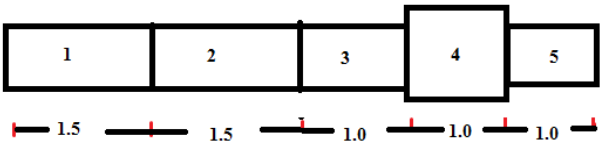

(d) Pile 4

Fig. 7 Discretized specimen for SFEM

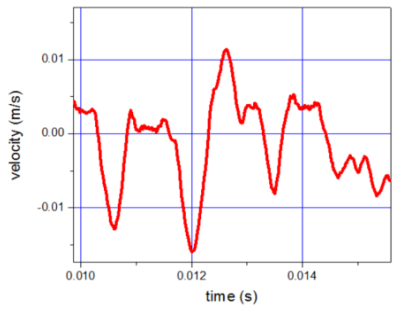

(a) Pile 1

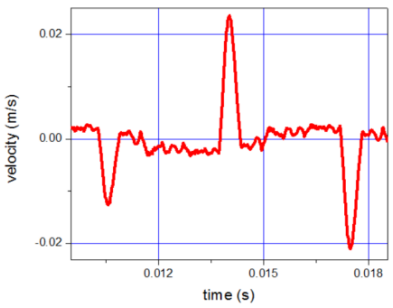

(b) Pile 2

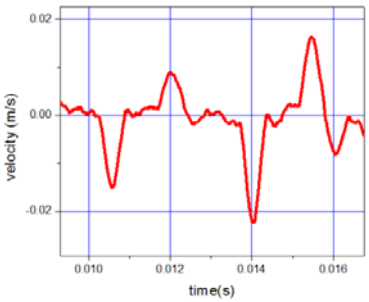

(c) Pile 3

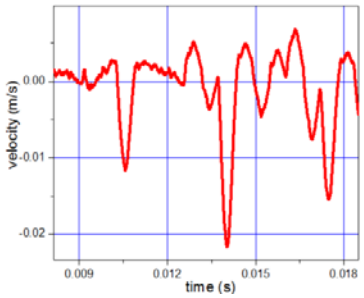

(d) Pile 4

Fig. 8 Numerically obtained velocity time response from SFEM

Table 2 Numerical results obtained from elementary rod theory (SFEM)

Model	Incident (s)	Damage reflection (s)	Location (m)	Toe reflection (s)	Location (m)
Pile 1	0.01026	0.01108	3.08	0.01181	5.8
Pile 2	0.01026	0.01148	4.58	0.01202	6.6
Pile 3	0.01026	0.01107	3.04	0.01202	6.6
Pile 4	0.01026	0.01146	4.50	0.01200	6.5

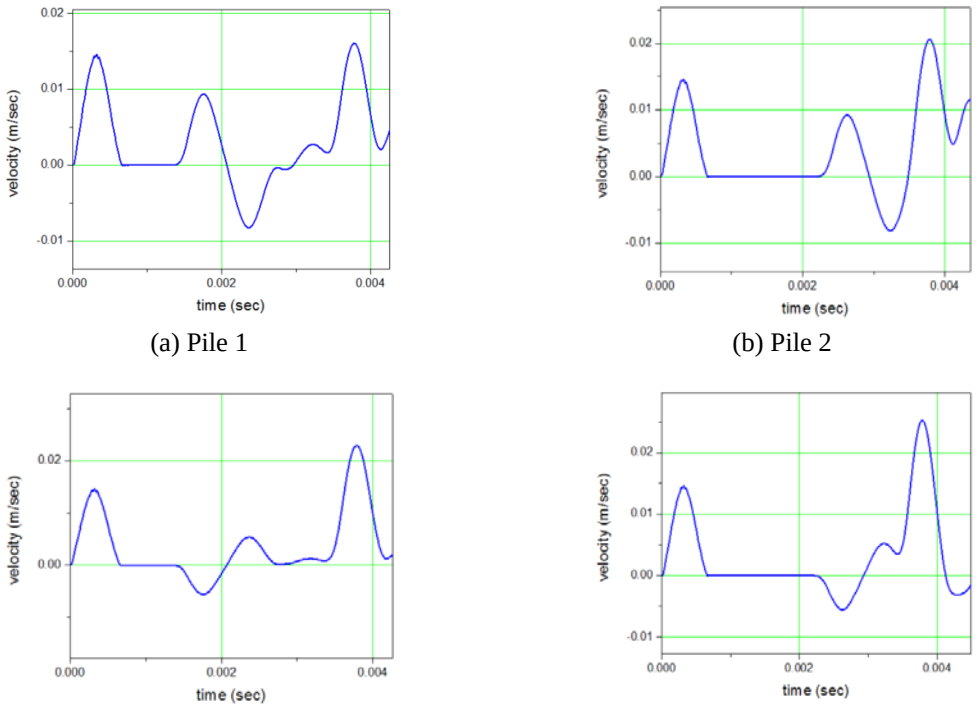

(a) Pile 1 (b) Pile 2

(c) Pile 3 (d) Pile 4

Fig. 9 Velocity response obtained from analytical results using SFEM

Table 3 Numerical results obtained from love rod theory (SFEM)

Specimen name	Incident (ms)	Damage reflection (ms)	Location(m)	Toe reflection (ms)	Location(m)
Pile 1	0.00868	0.01001	2.50	0.01202	6.2
Pile 2	0.01041	0.01255	4.01	0.01371	6.1
Pile 3	0.01662	0.01796	2.51	0.01983	6.1
Pile 4	0.01043	0.01113	1.30	0.01374	6.2

4.3.3 Comparison of analytical and experimental results for pile with damage

The acceleration responses obtained from analytical studies at toe region are shown in Fig. 10. For better understanding of the results, comparison is made for both analytical and experimental results and is shown in Fig. 11.

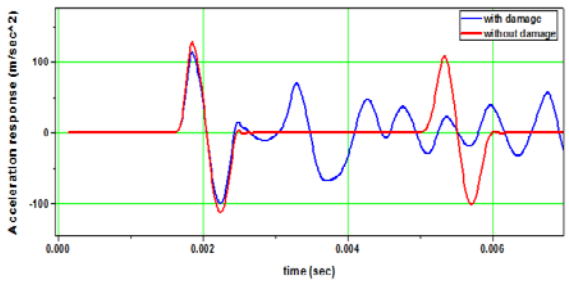

(a) Pile 1

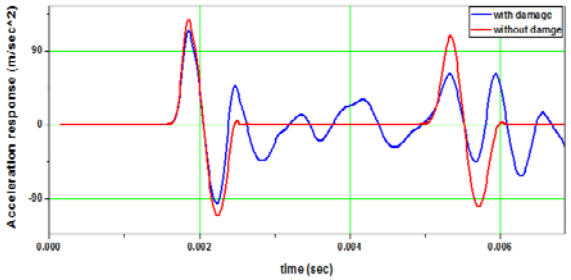

(b) Pile 2

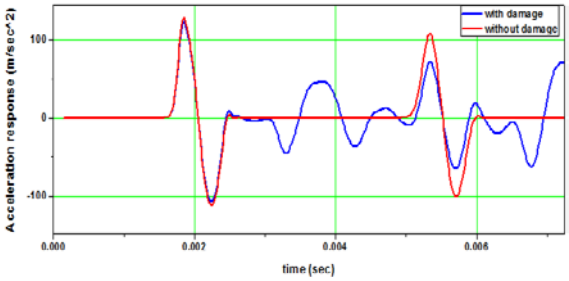

(c) Pile 3

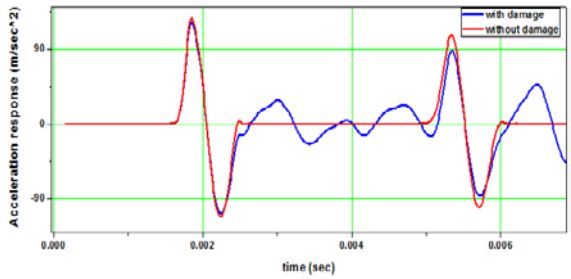

(d) Pile 4

Fig. 10 Analytical plot for comparison of pile with no defect and with damage

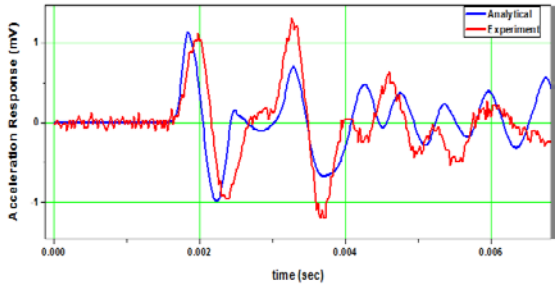

(a) Pile 1

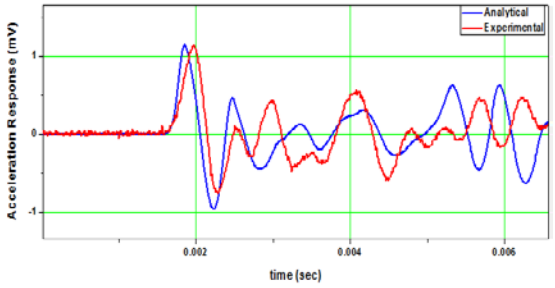

(b) Pile 2

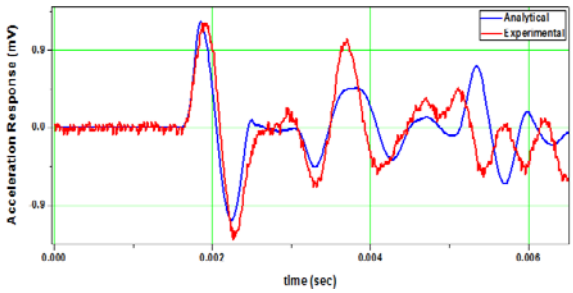

(c) Pile 3

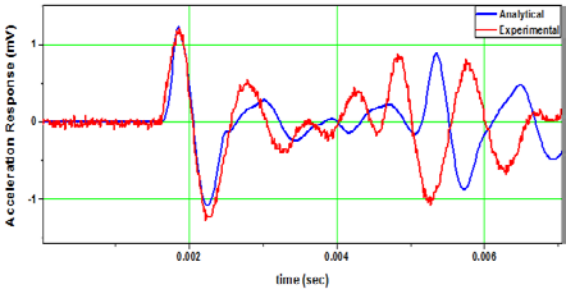

(d) Pile 4

Fig. 11 Comparison of Analytical and experimental results for pile with damage

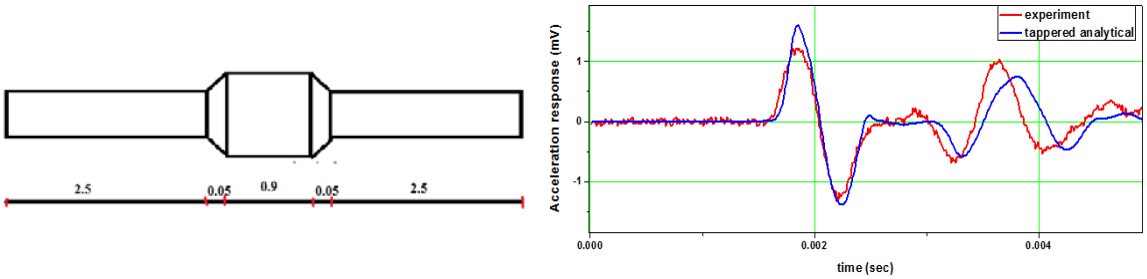

(a) (b)

Fig. 12 Comparison plot between experimental and tapered analytical result

- For the test specimen, the location of damage is at 2.5 m, 4 m, and 1m and from the response obtained it is approximately a quite good damage reflection. For all cases, the toe location is very well identified as it is approximately 6 m (pile length).
- By comparing the analytical and experimental responses it is clear that values are in good agreement. The plots show that the reflected wave profile is different for reduced and increased c/s area.
- A sign change is observed in the reflected acceleration pulse received from the bulged c/s area, at a time difference which is exactly equal to the ($2*L_1/c$), where L_1 indicates the distance between the head of the pile and starting point of bulged area.
- There is no sign change in case of reduced area. Here also, the time difference is equal to the ($2*L_1/c$) where L_1 indicates the distance between the head of the pile and starting point of the reduced area.
- Pulse shape being preserved in the reflected pulses in the un-damaged prismatic pile, coming out of the analytical study illustrates the phenomenon of uniform wave propagation.

In order to match the experimental response exactly to the analytical results, the concept of wave mechanics is utilized. The angle of stress flow at the sudden discontinuity will be in the range of 45° to 60°. Analytical match with the experimental results are achieved after a suitable length of transition area quantified by the angle of stress flow (taken as 45°) is modeled in the numerical studies (Fig. 12(a)). Analytical match with the experimental results can be achieved after a suitable length of transition area quantified by the angle of stress flow in the numerical studies as shown in Fig. 12(b).

5. Analytical investigations using ABAQUS

As there are many methods available for damage identification and detection, studying the results from those methods is of equal importance as to know the location and severity of damage. The analytical investigations are performed using ABAQUS software – dynamic explicit analysis. Five pile elements namely No Damage pile, Pile1, Pile 2, Pile 3, and Pile 4 are modeled in the ABAQUS and dynamic explicit analysis was performed on the piles by using Pulse-echo method and Pitch-catch configuration methods. All the pile elements are having a length of 6 m. No damage Pile is of Size 0.2 m × 0.2 m along the full length. The remaining pile elements namely Pile 1, Pile 2, Pile 3, and Pile 4 are already described in the experimental part. All the piles are

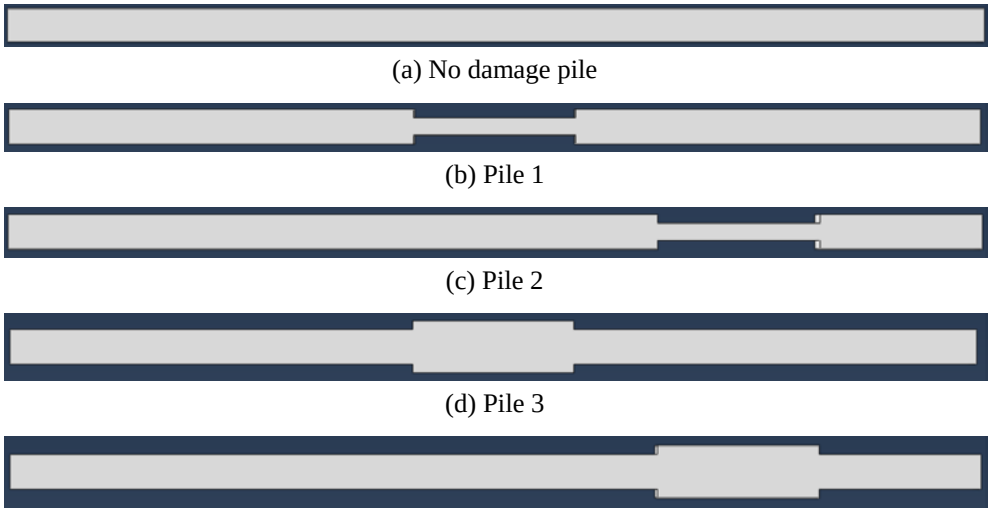

(a) No damage pile

(b) Pile 1

(c) Pile 2

(d) Pile 3

(e) Pile 4

Fig. 13 Front view of pile elements modeled in ABAQUS

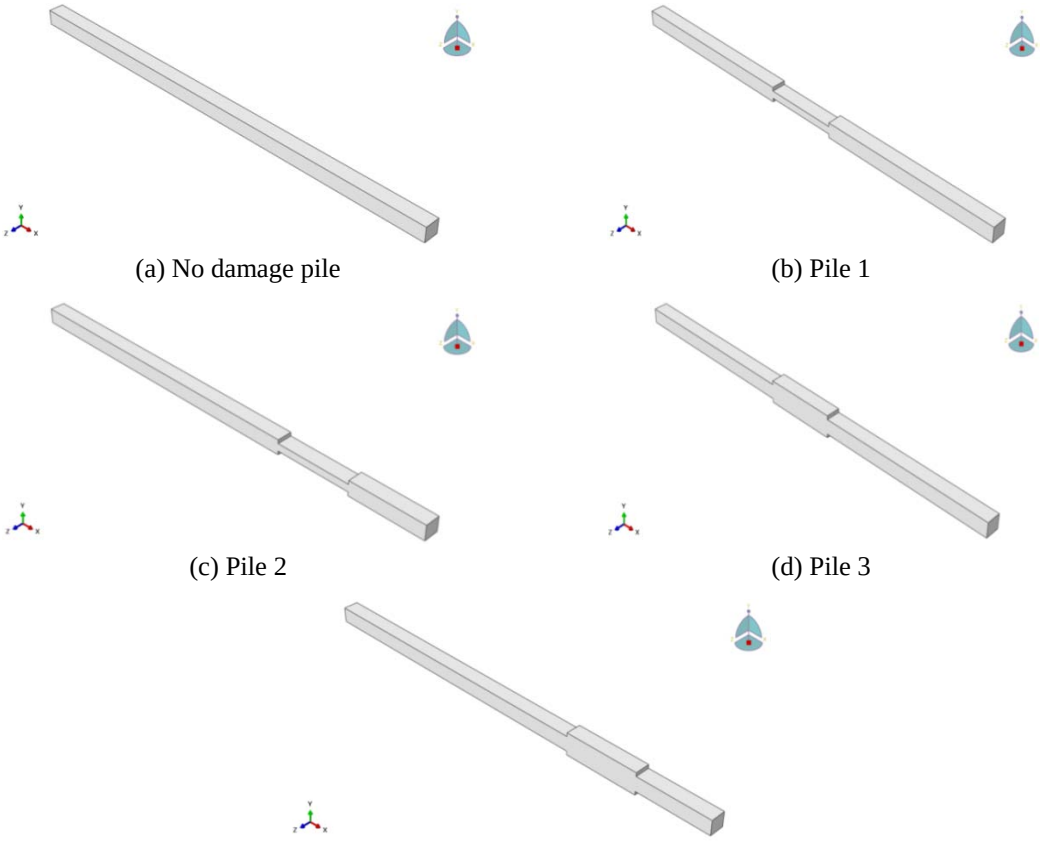

(a) No damage pile

(b) Pile 1

(c) Pile 2

(d) Pile 3

(e) Pile 4

Fig. 14 3-D view of the pile elements modeled in ABAQUS

made of M30 grade concrete and Fe415 steel. Poisson's ratio is assumed as 0.15 for concrete and the same properties are used in the modeling in ABAQUS. All the elements were created in 3D Modeling space and the type of the element is considered as deformable with solid extrusion shape. The approximate global size of the mesh is considered as 0.01.The load is applied axially to the head and the reflected waves from the damages or defects or toe are sensed by the sensors present at the head and toe of the pile. Consider, Wave speed, c = 3310 m/sec. The modeled piles are shown in Figs. 13 and 14.

5.1 Pulse-echo method

In this method, the head of the pile is given axial load at center, and the sensor is located at the head. When the pile element is loaded axially, downward compressive waves are generated which travels with a velocity (c) along the pile and reflects from damages or defects or toe. The sensor which is located at the head of the pile senses the waves and the velocity time profiles are noted down for the whole duration. From the reflected wave time and with the help of velocity of the wave, the damage location can be obtained. The input excitation which was given at the head of the pile element is shown in Fig. 15. The velocity-time profiles obtained in this method are presented in Fig. 16. The location of the damages based on the reflected times and wave velocity are tabulated in Table 4.

In Figs. 16(b)-(c), after the initial damage there is decrement in the c/s at some distance and thus the wave travels upwards, after 1 m length again the c/s increases and thus the wave travels in the downward direction. Similarly, in Fig. 16(d)-(e) after the initial damage there comes the increment in the c/s at some distance and thus the wave travels downwards, after 1 m length again

Table 4 Damage locations identified by pulse-echo method: ABAQUS results

Specimen name	Incident (ms)	Damage reflection 1 (ms)	Location (m)	Damage reflection 2 (ms)	Location (m)	Toe reflection (ms)	Location (m)
No damage	0	--	--	--	--	3.6	5.955
Pile 1	0	1.48	2.45	2.14	3.54	3.57	5.905
Pile 2	0	2.38	3.95	3.02	4.95	3.59	5.945
Pile 3	0	1.50	2.48	2.12	3.50	3.60	5.955
Pile 4	0	2.38	3.94	3.03	5.01	3.57	5.915

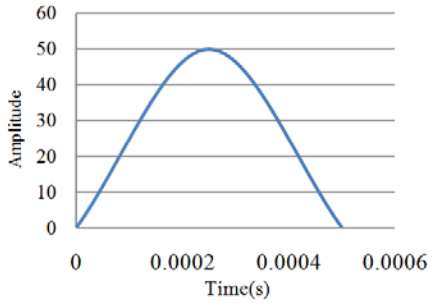

Fig. 15 Input excitation

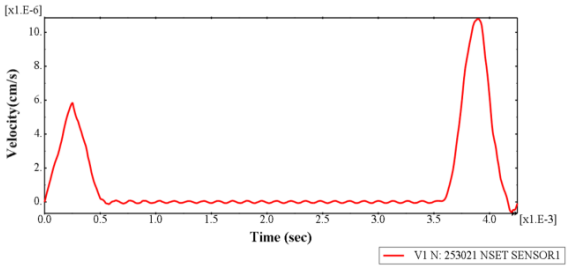

(a) No damage pile

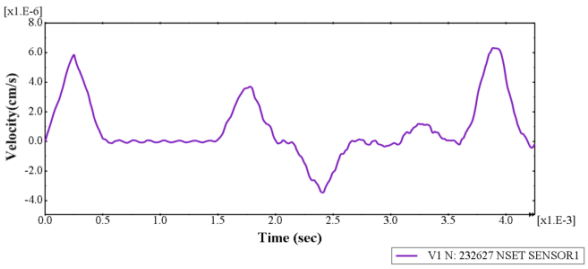

(b) Pile 1

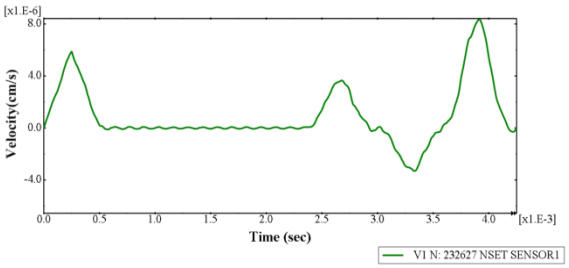

(c) Pile 2

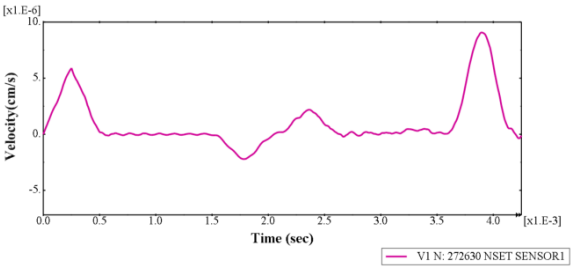

(d) Pile 3

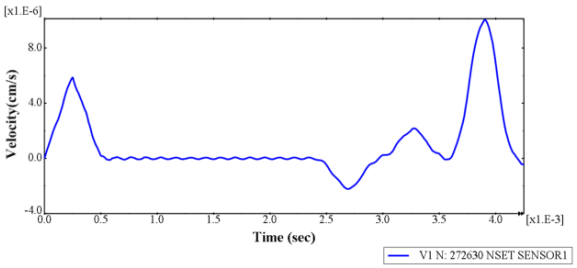

(e) Pile 4

Fig. 16 Velocity-time profilesobtained from pulse-echo method

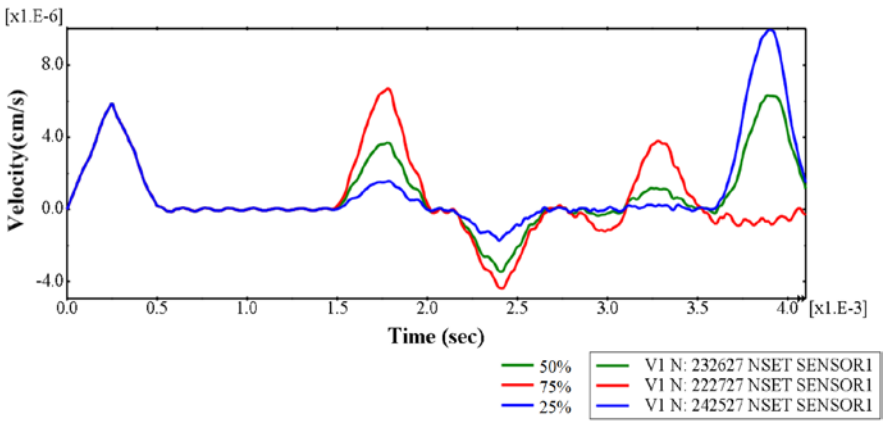

Fig. 17 Velocity time profiles for reductions in c/s area

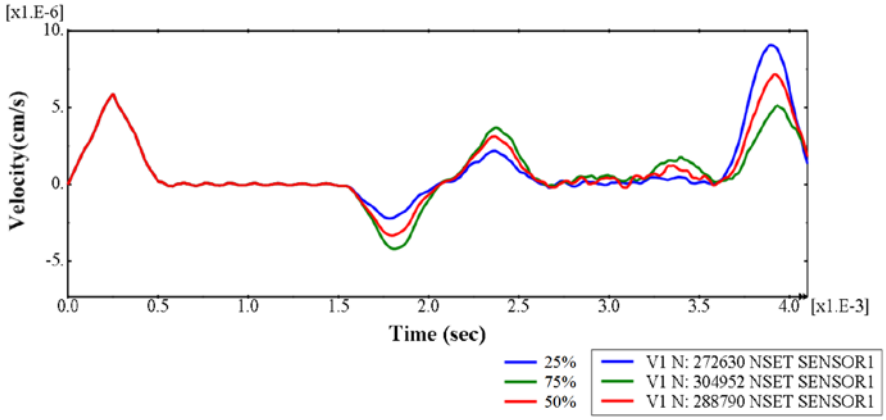

Fig. 18 Velocity time profiles for increase in c/s area

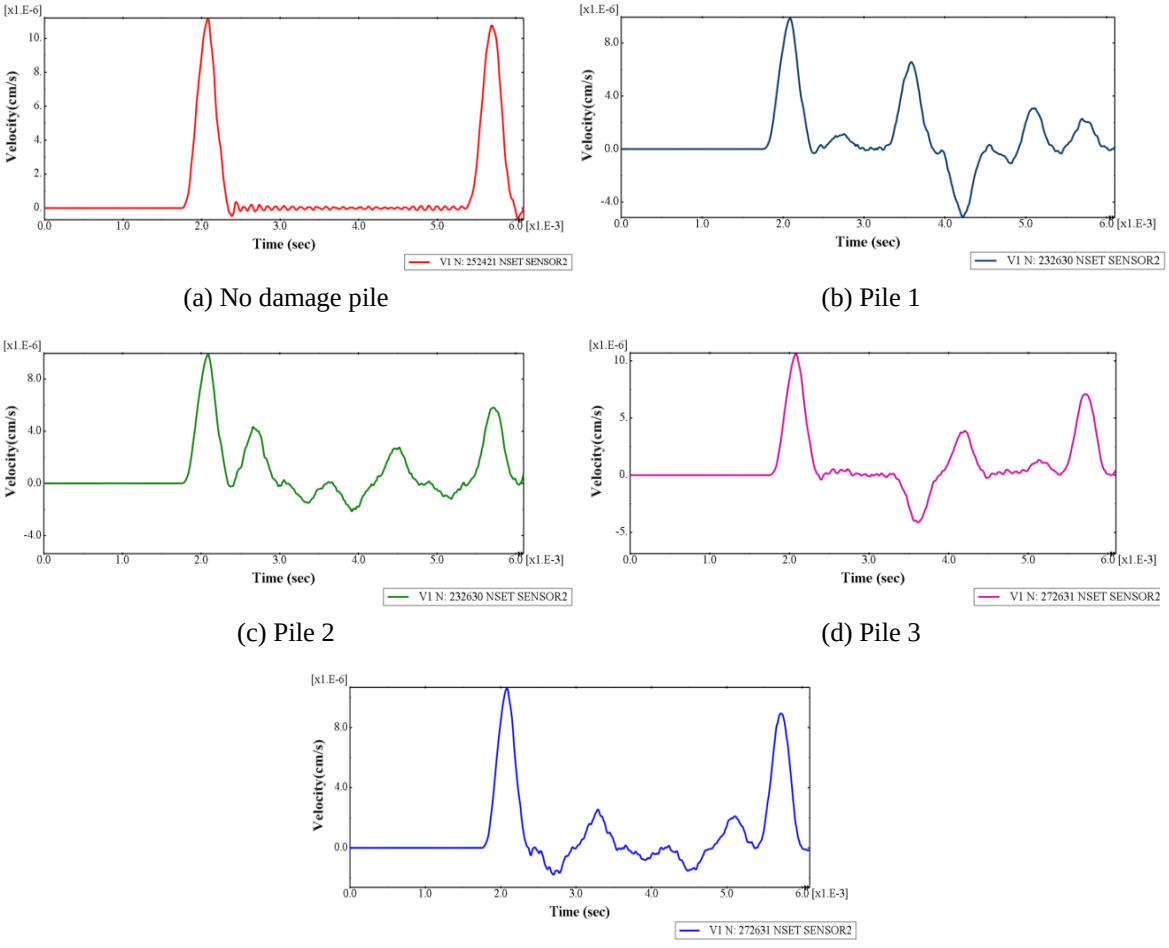

(a) No damage pile

(b) Pile 1

(c) Pile 2

(d) Pile 3

(e) Pile 4

Fig. 19 Velocity-time profiles obtained from Pitch-catch configuration method

Table 5 Damage locations identified by pitch-catch configuration method: ABAQUS results

Specimen name	Incident (ms)	Damage reflection 1 (ms)	Location (m)	Damage reflection 2 (ms)	Location (m)	Toe reflection (ms)	Location (m)
No damage	1.755	--	--	--	--	5.39	6.01
Pile 1	1.755	3.31	2.57	3.89	3.54	5.43	6.08
Pile 2	1.755	2.40	1.07	2.98	2.03	5.37	5.98
Pile 3	1.755	3.28	2.53	3.90	3.54	5.40	6.03
Pile 4	1.755	2.43	1.12	3.02	2.10	5.39	6.02

the c/s decreases and thus the wave travels in the upward direction. All the damage locations are obtained accurately with +/- 0.15 m precision.

For further investigation on the damages, models with 25%, 50%, and 75% reduction in area (Pile 1) and increase in the area (Pile 3) are studied and the velocity time graphs for them are shown in Figs. 17 and 18 respectively. It is clear that as the percentage increase or reductions in c/s are is more, the wave energy is more reduced and thus, the toe reflection peak is decreased.

5.2 Pitch-catch configuration method

In this method, the pile is struck at the head and the accelerometers are kept at the toe and the response is measured at the toe. The input excitation is shown in Fig. 15. The velocity time profiles obtained from the pitch-catch configuration method are shown in Fig. 19. As the sensor is present at the pile toe, the initial damage is not identified immediately and thus gives a peak after some time. Now the wave reflects from the pile toe and starts to propagate. Whenever it encounters a reduction or increase in c/s, it reflects back and is sensed by the sensor present at toe.

The time taken for reflection is noted down and by using this time and velocity, the damage locations are identified and are tabulated in Table 5. It is clear that in pitch-catch configuration method all the damages are identified accurately with +/- 0.15 m variation.

6. Conclusions

Damage identification under circumstances of non-dispersive wave propagation is a simpler task as compared to non-uniform flexural wave propagation because until reflections from damages or boundaries are encountered the shape of the transient pulse is conserved and the response is quiescent. In this paper damage identification of a pile element using axial wave propagation technique is studied through experimental testing (using pulse-echo and pitch-catch configuration methods) and numerical simulations using Spectral finite element method (SFEM) and ABAQUS dynamic explicit analysis. The wave scattering from elements of impedance change (impedance is analogous to dynamic stiffness and given as force per unit velocity) is used as a measure to identify a damage location and its magnitude. The wave scattering denotes both wave reflection (coming back to the source) and wave refraction (going away from source).In specific, the damages are detected by analyzing the reflections recorded using accelerometers and velocity of wave. The increase in the magnitude of the reflected pulses with increasing damage can be calibrated to quantify the damage magnitude. Analytical match with the experimental results are

achieved after a suitable length of transition area quantified by the angle of stress flow is modeled in the numerical studies. Pulse shape being preserved in the reflected pulses in the un-damaged prismatic beam, coming out of the analytical study illustrates the phenomenon of uniform wave propagation. The results obtained from SFEM and ABAQUS dynamic explicit analysis are compared with experimental results and are in good agreement. So, the proposed SFEM method is suitable and compatible for damage detection. It is suggested that the presented approach shall be suitable for exact damage detection, as the impedance around the structural discontinuity varies and so does the energy of propagating and reflecting waves.

Acknowledgments

The paper is published with the approval of Director, CSIR-SERC. The second and fourth authors thank for the tacit guidance of Tapas Kamakshi, Guru Ramana and Maha Periyava.

References

Ai, D., Zhu, H. and Luo, H. (2016), "Sensitivity of embedded active PZT sensor for concrete structural impact damage detection", *Constr. Build. Mater.*, **111**, 348-357.

Akbaş, Ş.D. (2014a), "Wave propagation analysis of edge cracked circular beams under impact force", *PloS one*, **9**(6), e100496.

Akbaş, Ş.D. (2014b), "Wave propagation analysis of edge cracked beams resting on elastic foundation", *Int. J. Eng. Appl. Sci.* (*IJEAS*), **6**(1), 40-52.

Akbaş, Ş.D. (2016), "Wave propagation in edge cracked functionally graded beams under impact force", *J. Vib. Control*, **22**(10), 2443-2457.

Bahrami, A. and Teimourian, A. (2015), "Nonlocal scale effects on buckling, vibration and wave reflection in nanobeams via wave propagation approach", *Compos. Struct.*, **134**, 1061-1075.

Barbieri, E., Cammarano, A., De Rosa, S. and Franco, F. (2009), "Waveguides of a composite plate by using the spectral finite element approach", *J. Vib. Control*, **15**, 347-367.

Bently, D.E. and Hatch, C.T. (2003), *Fundamentals of Rotating Machinery Diagnostics*, ASME Press, New York, NY, USA.

Bityurin, A.A. and Manzhosov, V.K. (2009), "Waves induced by the longitudinal impact of a rod against a steeped rod in contact with a rigid barrier", *J. Appl. Math. Mech.*, **73**, 162-168.

Doyle, J.F. (1997), *Wave Propagation in Structures*: *Spectral Analysis Using Fast Discrete Fourier Transforms*, Springer, New York, NY, USA.

Eltaher, M.A., Khater, M.E. and Emam, S.A. (2016), "A review on nonlocal elastic models for bending, buckling, vibrations, and wave propagation of nanoscale beams", *Appl. Math. Model*, **40**(5), 4109-4128.

Farrar, C.R. and Lieven, N.A.J. (2007), "Damage prognosis: the future of structural health monitoring", *Phil. Trans. R. Soc.*, **365**(1851), 623-632.

Farrar, C.R. and Worden, K. (2007), "An introduction to structural health monitoring", *Phil. Trans. R. Soc.*, **365**(1851), 303-315.

Feng, Q., Kong, Q. and Song, G. (2016), "Damage detection of concrete piles subject to typical damage types based on stress wave measurement using embedded smart aggregates transducers", *Measurement*, **88**, 345-352.

Frikha, A., Treyssede, F. and Cartraud, P. (2011), "Effect of axial load on the propagation of elastic waves in helical beams", *Wave Motion*, **48**(1), 83-92.

Gan, C., Wei, Y. and Yang, S. (2014), "Longitudinal wave propagation in a rod with variable cross-section", *J. Sound Vib.*, **333**(2), 434-445.

Gan, C., Wei, Y. and Yang, S. (2016), "Longitudinal wave propagation in a multi-step rod with variable

cross-section", *J. Vib. Control*, **22**(3), 837-852.
Gopalakrishnan, S. (2000), "A deep rod finite element for structural dynamics and wave propagation problems", *Int. J. Numer. Meth. Eng.*, **48**(5), 731-744.
Gopalakrishnan, S. and Doyle, J.F. (1994), "Wave propagation in connected wave guides of varying cross section", *J. Sound Vib.*, **175**(3), 347-363.
Gopalakrishnan, S. and Doyle, J.F. (1995), "Spectral super-elements for wave propagation in structures with local non uniformities", *Comput. Method Appl. M.*, **121**(1-4), 77-90.
Guo, S. and Yang, S. (2012), "Wave motions in non-uniform one-dimensional waveguides", *J. Vib. Control*, **18**(1), 92-100.
He, W.Y. and Zhu, S. (2015), "Adaptive-scale damage detection strategy for plate structures based on wavelet finite element model", *Struct. Eng. Mech., Int. J.*, **54**(2), 239-256.
He, W.Y., Zhu, S. and Ren, W.X. (2014), "A wavelet finite element-based adaptive-scale damage detection strategy", *Smart Struct. Syst., Int. J.*, **14**(3), 285-305.
Hibbitt, H., Karlsson, B. and Sorensen, P. (2011), "Abaqus analysis user's manual version 6.10", *Dassault Systèmes Simulia Corp.*: Providence, RI, USA.
Kisa, M. and Gurel, M.A. (2007), "Free vibration analysis of uniform and stepped cracked beams with circular cross sections", *Int. J. Eng. Sci.*, **45**(2), 364-380.
Kocatürk, T., Eskin, A. and Akbaş, Ş.D. (2011), "Wave propagation in a piecewise homogenous cantilever beam under impact force", *Int. J. Phys. Sci.*, **6**(16), 3867-3874.
Krawczuk, M. (2002), "Application of spectral beam finite element with a crack and iterative search technique for damage detection", *Finite Elem. Anal. Des.*, **38**(6), 537-548.
Krawczuk, M., Palacz, M. and Ostachowicz, W. (2003), "The dynamic analysis of a cracked Timoshenko beam by the spectral element method", *J. Sound Vib.*, **264**(5), 1139-1153.
Krawczuk, M., Grabowska, J. and Palacz, M. (2006), "Longitudinal wave propagation. Part I- Comparison of rod theories", *J. Sound Vib.*, **295**(3), 461-478.
Lakshmanan, N., Raghuprasad, B.K., Gopalakrishnan, N., Sathishkumar, K. and Murthy, S.G.N. (2010), "Detection of contiguous and distributed damage through contours of equal frequency change", *J. Sound Vib.*, **329**(9), 1310-1331.
Lee, S.K., Mace, B.R. and Brennan, M.J. (2007), "Wave propagation, reflection and transmission in non-uniform one-dimensional waveguides", *J. Sound Vib.*, **304**(1), 31-49.
Liu, K., Li, X. and Sun X. (1997), "A numerical method for axisymmetric wave propagation problem of anisotropic solids", *Comput. Methods Appl. Mech. Engrg.*, **145**(1-2), 109-116.
Mahapatra, D.R. and Gopalakrishnan, S. (2003), "A spectral finite element model for analysis of axial–flexural–shear coupled wave propagation in laminated composite beams", *Comput. Struct.*, **59**(1), 67-88.
Ostachowicz, W. (2008), "Damage detection of structures using spectral finite element method", *Comput. Struct.*, **86**(3), 454-462.
Ostachowicz, W., Krawczuk, M., Zak, A. and Kudela, P. (2006), "Damage detection in elements of structures by the elastic wave propagation method", *Compt. Asst. Mech. Eng. Sci.*, **13**, 109-124.
Palacz, M. and Krawczuk, M. (2002), "Analysis of longitudinal wave propagation in a cracked rod by the spectral element method", *Comput. Struct.*, **80**(24), 1809-1816.
Palacz, M., Krawczuk, M. and Ostachowicz, W. (2005a), "The spectral finite element model for analysis of flexural–shear coupled wave propagation: Part 1: Laminated multilayer composite beam", *Compos. Struct.*, **68**(1), 37-44.
Palacz, M., Krawczuk, M. and Ostachowicz, W. (2005b), "The spectral finite element model for analysis of flexural-shear coupled wave propagation. Part 2: Delaminated multilayer composite beam", *Compos. Struct.*, **68**(1), 45-51.
Rao, G.V.R., Davis, T.T., Sreekala, R., Gopalakrishnan, N., Iyer, N.R. and Lakshmanan, N. (2015), "Damage identification through wave propagation and vibration based methodology for an axial structural element", *J. Vib. Eng. Tech.*, **3**(4), 383-399.
Saravanan, T.J. Gopalakrishnan, N. and Rao, N.P. (2015a), "Damage detection in structural element through propagating waves using radially weighted and factored RMS", *Measurement*, **73**, 520-538.

Saravanan, T.J., Rao, N.P. and Gopalakrishnan, N. (2015b), "Experimental and numerical investigation on longitudinal wave propagation in rod with structural discontinuity", *J. Struct. Eng.* (*India*), **42**(1), 1-7.
Saravanan, T.J., Gopalakrishnan, N. and Rao, N.P. (2016), "Detection of damage through coupled axial–flexural wave interactions in a sagged rod using the spectral finite element method", *J. Vib. Control*. DOI: 10.1177/1077546316630855
Shull, P.J. (2002), *Non-Destructive Evaluation Theory, Techniques, and Applications*, Marcel Dekker Inc., New York, NY, USA.
Tian, J., Li, Z. and Su, X. (2003), "Crack detection in beams by wavelet analysis of transient flexural waves", *J. Sound Vib*., **261**(4), 715-727.
Worden, K. and Dulieu-Barton, J.M. (2004), "An overview of intelligent fault detection in systems and structures", *Int. J. Struct. Health Monit*., **3**(1), 85-98.
Wu, Z.J. and Li, F.M. (2014), "Spectral element method and its application in analyzing the vibration band gap properties of two-dimensional square lattices", *J. Vib. Control*. DOI: 10.1177/1077546314531805
Yang, Z., Radzienski, M., Kudela, P. and Ostachowicz, W. (2016), "Two-dimensional modal curvature estimation via Fourier spectral method for damage detection", *Compos. Struct*., **148**, 155-167.
Zak, A. and Krawczuk, M. (2011), "Certain numerical issues of wave propagation modelling in rods by the spectral finite element method", *Finite Elem. Anal. Des*., **47**(9), 1036-1046.

CC